

Zoom-Whirl Orbits in Black Hole Binaries

James Healy¹, Janna Levin^{2,3}, and Deirdre Shoemaker⁴

¹ *Center for Gravitational Physics, The Pennsylvania State University, University Park, PA 16802*

² *Barnard College of Columbia University, Department of Physics and Astronomy, 3009 Broadway, New York, NY 10027*

³ *Institute for Strings, Cosmology, and Astroparticle Physics, Columbia University, New York, NY 10027 and*

⁴ *Center for Relativistic Astrophysics and School of Physics, Georgia Institute of Technology, Atlanta, GA 30332*

Zoom-whirl behavior has the reputation of being a rare phenomenon. The concern has been that gravitational radiation would drain angular momentum so rapidly that generic orbits would circularize before zoom-whirl behavior could play out, and only rare highly tuned orbits would retain their imprint. Using full numerical relativity, we catch zoom-whirl behavior despite dissipation. The larger the mass ratio, the longer the pair can spend in orbit before merging and therefore the more zooms and whirls seen. Larger spins also enhance zoom-whirliness. An important implication is that these eccentric orbits can merge during a whirl phase, before enough angular momentum has been lost to truly circularize the orbit. Waveforms will be modulated by the harmonics of zoom-whirls, showing quiet phases during zooms and louder glitches during whirls.

Kepler's laws describe closed elliptical planetary motions. A small relativistic correction accounts for the tiny, anomalous precession of Mercury's perihelion. If the sun is replaced by a black hole, the geodesic motions can zoom and whirl in an extreme form of precession – whirling around the center of mass in nearly circular inspiral before zooming out along elliptical leaves. Zoom-whirl behavior is characteristic of strong relativity and could potentially be detected in the harmonics of the gravitational waves generated.

There are astrophysical settings that could populate eccentric merges, such as dense galactic nuclei [1] or globular clusters [2, 3]. Consequently, it is an important astrophysical question to ask: Can zoom-whirl behavior, an intrinsically eccentric phenomenon, survive the dissipative drain of gravitational radiation? In this article we report on results of numerical relativity that show zoom-whirl behavior in comparable mass binaries, answering this question in the affirmative.

As there is no analytic description of the curved space-time around two black holes, we rely either on analytic approximations or on numerical relativity to describe comparable black hole pairs. Zoom-whirl behavior has been studied in extreme-mass ratio inspirals [4, 5, 6, 7] and was recently found in an analytic approximation, specifically conservative Post-Newtonian (PN) approximations to black hole binaries [8, 9]. Now we find zoom-whirl orbits in full numerical relativity of spinning pairs. Zoom-whirl behavior has already been found in numerical relativity for equal-mass, nonspinning binaries in [10]. In that work, the initial conditions were carefully tuned to find a special orbit, the separatrix between bound orbital motion and plunge. The separatrix is studied in detail in the PN approximation in [9] and an analytic solution for the separatrix in Kerr systems was found in [11, 12].

In this Letter we show that zoom-whirl behavior in spinning pairs is a common feature of eccentric orbits [8, 9, 11], despite dissipation. In particular, zoom-whirl orbits happen well away from the separatrices and so do not in general require fine tuning of initial conditions

(see also [13, 14]). Due to the computational expense of running these simulations, a full scan of parameters is not possible. To focus our investigation, we rely on analytic approximations to estimate good initial conditions and we then run full numerical simulations to easily locate zoom-whirl inspirals. The further utility of the analytic estimates is the transparency of interpretation.

The anatomy of zoom-whirl behavior was quantified in Ref. [15] where it was shown that every orbit of a given L can be described by one number that specifies the precession of the orbit per radial cycle from apastron to apastron. The amount by which an orbit will precess, that is, overshoot the previous apastron is

$$\Delta\phi_{precess} = 2\pi q \quad \text{where} \quad q = w + \frac{v}{z} \quad . \quad (1)$$

A perfectly periodic orbit looks like a closed 1-leaf clover or 2-leaf clover or 3-leaf clover, or z -leaf clover. And each periodic orbit corresponds to a rational q made up of w integer number of nearly circular whirls close to perihelion per leaf in the z -leaf clover. The vertex v is more subtle and indicates the order in which the z -leaves are traced out. So, a simple 3-leaf clover for instance is a $q = 1/3$ ($w = 0, v = 1, z = 3$) and precesses past the previous apastron by $\Delta\phi = 2\pi q = 2\pi/3$ per radial cycle. A 3-leaf clover that skips a leaf in the pattern each time corresponds to $q = 2/3$ ($w = 0, v = 2, z = 3$) and precesses by $\Delta\phi = 2\pi q = 4\pi/3$ per radial cycle. Therefore, q quantifies zoom-whirl behavior, the integer part signals the whirls per leaf and the fractional part signals the number and order of the leaves.

Another way to interpret the number is as the ratio of frequencies, $q = \omega_\phi/\omega_r$, where ω_ϕ is the average of the angular frequency per radial cycle and $\omega_r = 2\pi/T_r$ where T_r is the time between apastron. For periodic orbits the frequencies are rationally related and the orbit will eventually close. Whirls accumulate near perihelion simply because the angular velocity is greatest on closest approach and the circumference smallest.

Generic orbits are not periodic and do not correspond

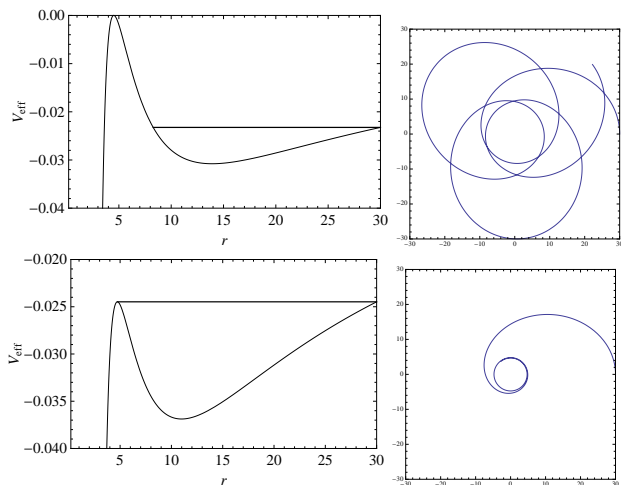


FIG. 1: The 3PN effective potential. Top: $L_{IBCO} \sim 4.4$. The straight line corresponds to the orbit $r_a = 30$. Bottom: $L \sim 4.1$, for which the orbit with $r_a = 30M$ is the separatrix.

to rational q . However, any generic orbit can be approximated by a nearby periodic, just as any irrational number can be approximated by a nearby rational number. Kepler’s ellipse corresponds to $q = 0$ since it does not precess at all. Mercury’s precessing orbit corresponds to $q \sim 10^{-7}$ since it precesses very little. Technically, zoom-whirl behavior corresponds to $q > 1$, so there is at least one whirl, although we will generally be interested in any substantial precession, say $q > 1/4$.

If angular momentum is fixed, q decreases monotonically with decreasing energy. However angular momentum decreases, along with energy, as gravitational radiation is emitted and the evolution of q will not necessarily be monotonic. In the case of comparable mass black hole pairs, q will change quickly due to the rapid losses to gravitational waves as evident in the simulations.

The range of zoom-whirl behavior is most easily targeted with an effective potential picture. In Ref. [9, 15] an effective potential method was used to describe the center-of-mass motion of black hole binaries in the conservative 3PN Hamiltonian description with spin-orbit coupling included. There it was shown that at the turning points of the orbital motion, the Hamiltonian itself is an effective potential and the motion can be read off as easily as interpreting a ball rolling along hills.

Consider the effective potential on the top left of Fig. 1 from the conservative 3PN Hamiltonian [9, 15, 16, 17]. There is clearly a minimum of that potential which defines a stable circular orbit. An orbit energetically above the stable circle will execute elliptical precessions as shown on the top right. Note these precessions are much more extreme than Mercury’s with $q > \frac{1}{3}$. It looks like a precession around a three leaf clover. The aperiodic orbit will eventually fill out an annulus.

Also evident is a maximum of the potential, an unstable circular orbit. For this angular momentum the unstable circular orbit is marginally, energetically bound

since V_{eff} just skims zero there, and has been called an innermost bound circular orbit (IBCO). An orbit at rest at infinity would asymptotically approach this circular orbit. And though initially of eccentricity one, $e = 1$, this orbit whirls an infinite number of times as it climbs the potential toward the unstable circle at the top. This separatrix is the infinite whirl orbit, $q = \infty$, and is also known as a homoclinic orbit of eccentricity one.

For angular momenta below this critical value, the unstable circular orbit marches down in energy. For each unstable circle, there is a corresponding separatrix of decreasing eccentricity. As an example, on the bottom of Fig. 1, the separatrix between bound motion and plunge has apastron $r_a = 30M$ and asymptotically approaches the unstable circular orbit in the infinite whirl limit. So this is the $q = \infty$ orbit for $L \sim 4.1$, where throughout we measure angular momentum in units of μM and $M = m_1 + m_2$ while $\mu = m_1 m_2 / M$. The homoclinic separatrix is plotted alongside the corresponding effective potential on the bottom right of Fig. 1.

We expect to see zoom-whirl behavior until the unstable circular orbit and the stable circular orbit merge at the ISCO (innermost stable circular orbit), the separatrix with $e = 0$. Quasi-circular inspiral plunges at the ISCO and so this inflection point in the effective potential has received preferential attention. However, orbits that maintain an eccentricity during inspiral will merge by rolling over the top of the potential, through a homoclinic separatrix, behavior we observe in our simulations.

Roughly then, for given external parameters $(m_2/m_1, \mathbf{S}_1, \mathbf{S}_2)$, zoom-whirl behavior should be sought in the range $L_{ISCO} < L < L_{IBCO}$. One more initial condition needs to be specified to define an orbit and that could be either the energy or the apastron. We’ll choose to fix the apastron. We’ll fill in the details for a fiducial example and then flush out more general trends we have observed.

The procedure is the following: (1) choose external parameters namely mass ratio and spins $(m_2/m_1, \mathbf{S}_1, \mathbf{S}_2)$, (2) render the effective potential for the 3PN Hamiltonian with spin-orbit coupling, (3) glean the range of L for which there will be zoom-whirl behavior and (4) run simulations for this range of initial conditions.

For our fiducial example we take mass ratio $m_2/m_1 = 1/3$ and spin magnitudes $S_1/m_1^2 = S_2/m_2^2 = 0.3$ with spins antialigned with the orbital angular momentum. Antialigned spins, like aligned spins, will retain the orbital motion in the equatorial plane making it easier to distinguish whirl precession. Other than the choice to retain equatorial motion for transparency, there is nothing special about the fiducial configuration. We consider a set of orbits all of which begin at apastron $r_a = 30M$. Since the simulations are so costly, we tighten the range to the more realistic values of angular momenta below L_{IBCO} and above the value of the angular momentum at which $r = r_a$ is the apastron of a homoclinic orbit. Specifically, we look between the values represented by the top and bottom of Fig. 1; $4.1 < L < 4.4$.

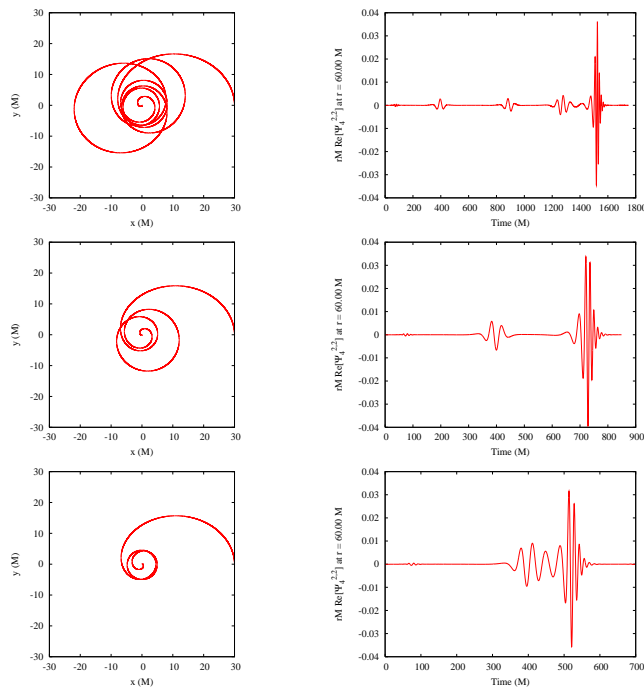


FIG. 2: The initial apastron is $r_a = 30M$. Left column, from the top, frame 1: $L = 4.10$ and the orbit rapidly moves through zoom-whirl cycles precessing by $> \pi$ ($q \sim 1/2$) between apastra. The orbit rapidly loses eccentricity but still merges with non-zero eccentricity. Frame 2: $L = 3.95$ and the orbit precesses by nearly $> 2\pi$ ($q \sim 1$) in the first radial cycle before merging. Frame 3: $L = 3.915$ and the orbit is very nearly homoclinic, precessing by $\sim 4\pi$ ($q \sim 2$) around the unstable circular orbit before radiative losses cause merger. Right Column: The gravitational waveforms versus simulation time were extracted at a finite radius of $60M$.

There are a few reasons why the actual range for numerical relativity will be offset from this 3PN prediction. For one, dissipation ensures that L changes as the orbit evolves. This is equivalent to the effective potential dropping as the orbit evolves. For another, the 3PN approximation is by definition not exact and its predictions are not to be overstated in this strong-field regime. Finally, although spin-orbit coupling is included in our analysis, spin-spin coupling terms are not included since they introduce angular dependencies that spoil the effective potential [9, 15]. Since spin-spin terms are small, their effect will presumably result in a small perturbation to our 3PN effective potential. Our range is intended only as a guide and apparently does well enough, as we'll see.

In between this range, all orbits with our external parameters ($m_2/m_1 = 1/3$, $S_1/m_1^2 = S_1/m_2^2 = 0.3$), antialigned, and an apastron of $r_a = 30M$, will show zoom-whirl behavior with $1/3 < q < \infty$. This is the story told by the conservative dynamics. To test the survival of zoom-whirl orbits under the dissipative effects of radiative reaction we turn to full numerical relativity now.

The runs in Fig. 2 were simulated using the Georgia Tech MayaKranc code that uses the same compu-

tational infrastructure and methodology as in previous studies [18, 19, 20, 21, 22], namely a Baumgarte-Shapiro-Shibata-Nakamura code with moving puncture gauge conditions [23, 24] using the Kranc code generator [25]. The black-hole encounters are initiated with Bowen-York initial data [26]. The black holes are located on the x -axis: bh_\pm are located at $x_+ = 7.5M$ and $x_- = -22.5M$ where $m_+ = 3M/4$ and $m_- = M/4$. The spatial finite differencing is sixth order. We used eleven levels of refinement with Carpet [27], a mesh refinement package in Cactus [28]. The finest resolution is $M/143$ and the outer boundary is at $287M$. The total initial orbital angular momentum, is varied between the values of 3.9 and 4.1. The range is shifted from the conservative PN value as expected, yet zoom-whirl behavior was comfortably found given that initial prediction.

Fig. 2 shows three different orbits and their waveforms corresponding to different initial values of L . The largest value of L shows zoom-whirl behavior characterized by $q \sim 1/2$ before merging. The middle value of L has a $q \sim 1$ while the smallest value of L we show is very close to the separatrix and whirls nearly twice. We caution that we are only loosely reading off these values since q is changing so rapidly during inspiral.

As expected, the pairs merge by rolling over the top of the effective potential (Fig. 1). We emphasize that the nearly circular pattern of the whirl phase is not equivalent to full circularization of the orbit. In other words, quite importantly, the orbits shown in Fig. 2 do not merge through the ISCO but rather roll over the top of the potential, merging through a whirl. To compare with the language in a previous paper [29], some of those eccentric orbits were circular because they merged through a whirl phase and not because they merged through the ISCO. This could be relevant for initial conditions for the ringdown phase.

The waveforms show distinctly quiet phases during the highly elliptical zooms followed by louder glitches during the nearly circular whirls. The distinctive spikes of zoom-whirls are directly related to their rational number q . This suggests that zoom-whirl orbits could be dug out of the data using algorithms suited for burst searches, perhaps in conjunction with more targeted template searches.

Fig. 3 plots the relative orbital separation of the black holes versus phase for our three cases of L . The plot illustrates the rapid merger of the black holes as L decreases. The figure also shows that inspiral ends and plunge begins in the simulations for radii $\sim 5M$. In line with the numerical results, the effective potential picture in Fig. 1 predicts whirls around periastron, $\sim 5M$, which is much less than the PN predicted value of the ISCO, $r_{ISCO} \sim 8.8M$, for a mass ratio of $1/3$ and these spins. The figure therefore confirms that the zoom-whirl pair merge near a whirl phase and not near the ISCO. The top line, corresponding to $L = 4.1$, shows the three zooms before merger that we see in frame 1 of Fig. 2. The bottom line, corresponding to $L = 3.915$ and frame 3 of Fig.

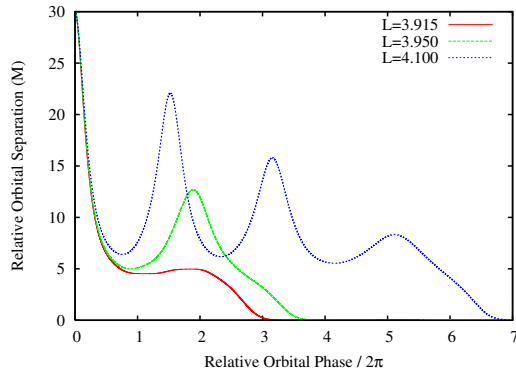


FIG. 3: The relative orbital separation in units of M plotted versus the orbital phase for the series of L in Fig. 2.

2 is almost homoclinic with no zooms, precessing around the unstable circular orbit before merging.

In general, we conclude from the PN approximation that zoom-whirl behavior has better odds at surviving dissipation and leaving a mark in the gravitational waveform for (1) more disparate values of m_2/m_1 because of

the slower dissipation time, (2) larger spin magnitudes, all else being equal, because of the greater frame dragging effect, (3) larger initial apastra because of the longer orbital lifetime. There is less zoom-whirl behavior in equal-mass nonspinning pairs, hence the importance of sticking closer to the separatrices [10]. Yet more generally, zoom-whirl orbits ought to extend down below the separatrices. In the future, we intend to extend this work by pushing the numerical simulations to large mass ratio and extracting a measure of \dot{q} .

For any zoom-whirl pair, the glitchy waveforms followed by longer quiescent phases are highly distinctive and beg for tailored search algorithms. Furthermore, the loud glitches could nudge these highly precessing orbits into an optimistic position for early direct detection.

Acknowledgements: The authors wish to acknowledge NSF grants AST-0908365, PHY-0925345, PHY-0653303 and TG-PHY060013N that supported this work. We also thank Ian Hinder, Frank Herrmann, Tanja Bode and Pablo Laguna for contributions to the `MayaKranc` code.

-
- [1] R. M. O’Leary, B. Kocsis, and A. Loeb, *Mon. Not. R. astr. Soc.* **395**, 2127 (2009).
- [2] B. Kocsis, M. E. Gaspar, and S. Marka, *Ap. J.* **648**, 411 (2006).
- [3] L. Wen, *Ap. J.* **598**, 419 (2003).
- [4] K. Glampedakis and D. Kennefick, *Phys. Rev. D* **66**, 044002 (2002).
- [5] L. Barack and C. Cutler, *Phys. Rev. D* **69**, 082005 (2004).
- [6] L. M. Burko and G. Khanna, *Europhys. Lett.* **78**, 60005 (2007).
- [7] R. Haas, *Phys. Rev. D* **75**, 124011 (2007).
- [8] J. Levin and R. Grossman, *Phys. Rev. D* **79**, 043016 (2009).
- [9] R. Grossman and J. Levin, *Phys. Rev. D* **79**, 043017 (2009).
- [10] F. Pretorius and D. Khurana, *Class. Quant. Grav.* **24**, S83 (2007).
- [11] J. Levin and G. Perez-Giz, *Phys. Rev. D* **79**, 124013 (2009).
- [12] G. Perez-Giz and J. Levin, *Phys. Rev. D* **79**, 124014 (2009).
- [13] U. Sperhake et al., *Phys. Rev. Lett.* **103**, 131102 (2009).
- [14] R. Gold, private communication, 2009.
- [15] J. Levin and G. Perez-Giz, *Phys. Rev. D* **77**, 103005 (2008).
- [16] A. Buonanno, Y. Chen, and T. Damour, *Phys. Rev. D* **74**, 104005 (2006).
- [17] T. Damour, *Phys. Rev. D* **64**, 124013 (2001).
- [18] M. C. Washik et al., *Phys. Rev. Lett.* **101**, 061102 (2008).
- [19] F. Herrmann, I. Hinder, D. Shoemaker, P. Laguna, and R. A. Matzner, *Astrophys. J.* **661**, 430 (2007).
- [20] F. Herrmann, I. Hinder, D. Shoemaker, and P. Laguna, *Class. Quant. Grav.* **24**, S33 (2007).
- [21] J. Healy, P. Laguna, R. A. Matzner, and D. M. Shoemaker, arXiv:0905.3914 (2009).
- [22] J. Healy et al., *Phys. Rev. Lett.* **102**, 041101 (2009).
- [23] M. Campanelli, C. O. Lousto, P. Marronetti, and Y. Zlochower, *Phys. Rev. Lett.* **96**, 111101 (2006).
- [24] J. G. Baker, J. Centrella, D.-I. Choi, M. Koppitz, and J. van Meter, *Phys. Rev. Lett.* **96**, 111102 (2006).
- [25] S. Husa, I. Hinder, and C. Lechner, *Computer Physics Communications* **174**, 983 (2006).
- [26] J. M. Bowen and J. W. York, *Phys. Rev. D* **21**, 2047 (1980).
- [27] E. Schnetter, S. H. Hawley, and I. Hawke, *Class. Quant. Grav.* **21**, 1465 (2004).
- [28] Cactus Computational Toolkit home page: <http://www.cactuscode.org>.
- [29] I. Hinder, B. Vaishnav, F. Herrmann, D. Shoemaker, and P. Laguna, *Phys. Rev. D* **77**, 081502 (2008).